

Current-induced metallic behavior in $\text{Pr}_{0.5}\text{Ca}_{0.5}\text{MnO}_3$ thin films: Competition between Joule heating and nonlinear conduction mechanisms

P. Padhan,¹ W. Prellier,^{1,*} Ch. Simon,¹ and R. C. Budhani²

¹Laboratoire CRISMAT, CNRS UMR 6508, 6 Bd du Maréchal Juin, F-14050 Caen Cedex, France

²Department of Physics, Indian Institute of Technology Kanpur, Kanpur-208016, India

(Received 16 March 2004; revised manuscript received 19 May 2004; published 7 October 2004)

Thin films of $\text{Pr}_{0.5}\text{Ca}_{0.5}\text{MnO}_3$ manganites exhibiting charge/orbital-ordered properties with colossal magnetoresistance have been synthesized by the pulsed laser deposition technique on both (100)- SrTiO_3 and (100)- LaAlO_3 substrates. The effects of current-induced metallic-behavior of the films are investigated as a function of the temperature and the magnetic field. Calculations based on a heat transfer model across the substrate, and our resistivity measurements reveal effects of Joule heating on charge transport over certain ranges of temperatures and magnetic fields. Our results also indicate that a nonlinear conduction, which cannot be explained by homogeneous Joule heating of the film, is observed when the material is less resistive ($<10^{-2} \Omega\cdot\text{cm}$). The origin of this behavior is explained with a model based on local thermal instabilities associated with phase-separation mechanism and a change in the long range charge-ordered state.

DOI: 10.1103/PhysRevB.70.134403

PACS number(s): 75.47.Gk, 75.70.Ak, 71.30.+h, 81.15.Fg

Mixed valence manganites exhibit several fascinating phenomena such as colossal magnetoresistance (CMR), spin polarization, ordering of charge, orbital and spin of Mn^{3+} and Mn^{4+} ions, and electronic phase separation.^{1,2} Charge/orbital-ordering (CO/OO) phenomena in particular have been seen when the dopant concentration (x) is close to the commensurate value $x=0.5$ in the reduced bandwidth systems. The charge-ordering gap in these systems collapses upon application of external perturbation like magnetic field, electric field, high pressure, optical radiation and electron irradiation.³ This results in a metal-like transport below the charge-ordering transition temperature (T_{CO}). For example, electric field leads to a nonlinear transport with hysteresis and switching depending on current, temperature and magnetic field history. These effects observed in different charge-ordered manganite systems, are attributed to the formation of conducting ferromagnetic regions within the antiferromagnetic medium.⁴⁻¹¹ In fact, the transport in these systems is often interpreted in terms of spin polarized tunneling conduction across the insulating phase and a percolative conduction mechanism. However, other explanations can be found in the literature, and some of them are listed below. For example, Guha *et al.*⁵ have attributed their observations of a nonlinear transport in $\text{Nd}_{0.5}\text{Ca}_{0.5}\text{MnO}_3$ thin films to depinning of the charge/orbital-ordered state. In contrast, Tokura *et al.*⁶ have suggested that the electric field may directly influence the direction of the orbital ordering in the highly insulating state and alter the magnetic state. Moreover Stankiewicz *et al.*⁷ have suggested the formation of a mixed state that is less resistive and highly magnetized than the initial charge-order state. Furthermore, Markovich *et al.*¹⁰ have suggested the condensate effect of charge density waves or spin density waves to the increase in nonlinear conduction observed in $\text{Pr}_{0.8}\text{Ca}_{0.2}\text{MnO}_3$.

In this article, we report the effects of electric current on the transport properties of $\text{Pr}_{0.5}\text{Ca}_{0.5}\text{MnO}_3$ (PCMO) thin films. The objective of this paper is to develop an understanding of the current-induced decrease of the resistivity in

these materials. Thus, we have performed detailed measurements of resistivity as a function of current and temperature in the presence or absence of a magnetic field. Our data reveal that Joule heating effects and nonlinear conduction of a fundamental nature are observed depending on temperature and the value of the resistivity. The origin of this behavior is explained with a model based on a phase separated medium.

Thin films ($\sim 800 \text{ \AA}$) of PCMO are grown on (100)-oriented SrTiO_3 (STO) and LaAlO_3 (LAO) substrates using pulsed laser deposition technique. More details of deposition, x-ray diffraction, and magnetotransport studies on PCMO are described elsewhere.^{11,12} The epitaxy and texture of these films were confirmed by x-ray diffraction using Seifert XRD 3000P and Philips MRD X'pert. The four-probe resistivity (ρ) measurements were performed using nanovoltmeter (Keithley 182), current source (Keithley 236 source measure unit) in the cryostat of a Physical Properties Measurement System (PPMS) supplied by Quantum Design USA as a function of the temperature (T) and magnetic field (H). For magnetization measurements, we have used the Quantum Design SQUID magnetometer. The sample was cooled to a desired temperature from room temperature in the absence of electric and magnetic fields to perform transport measurements. The magnetic field was applied parallel to the substrate plane.

The pseudocubic lattice parameter of bulk PCMO is $\sim 3.802 \text{ \AA}$,¹³ which is larger than the lattice parameter of LAO (3.79 \AA) and smaller than the lattice parameter of STO (3.905 \AA). These lattice parameters indicate that these PCMO films on LAO will be under in-plane compression whereas on STO the in-plane stress will be expansive. Also, the lattice mismatch of PCMO with STO (3.77 \AA) is larger as compared to that with LAO (3.839 \AA). The different state of stress in the 800 \AA thick films of PCMO on STO and LAO is not distinctive in the zero-field temperature-dependent resistivity shown in Figs. 1(a) and 1(b). For example, the zero-field cooled (ZFC) resistivity of PCMO on STO below room temperature shows thermally activated be-

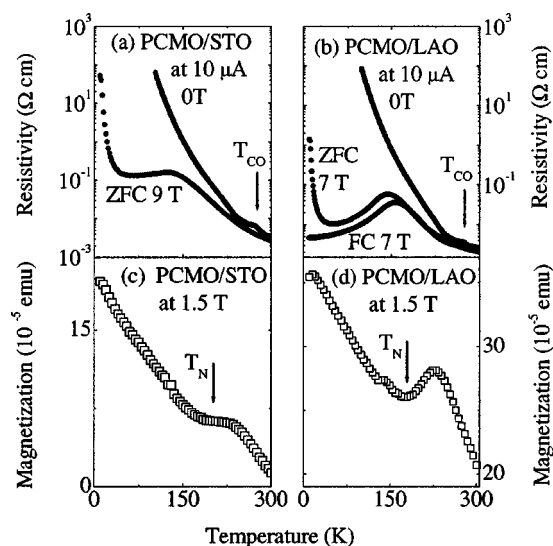


FIG. 1. (a) Zero-field-cooled temperature dependent resistivity of $\text{Pr}_{0.5}\text{Ca}_{0.5}\text{MnO}_3$ deposited on (001) oriented STO at 0 and 9 Tesla magnetic field at $10 \mu\text{A}$ current. (b) Zero-field-cooled and field-cooled temperature dependent resistivity of PCMO deposited on (001) oriented LAO at 0 and 7 Tesla magnetic field at $10 \mu\text{A}$ current. Panel (b) and (c) show the field-cooled magnetization of PCMO on STO and LAO, respectively, at 1.5 Tesla magnetic field at various temperature.

havior down to ~ 100 K with an activation energy (E_a) of 0.29 eV, which is slightly larger than its bulk value [0.2 eV (Ref. 14)]. Similar values are found for LAO (0.31 eV) in agreement with the zero-field dependence of the resistivity reported in Figs. 1(a) and 1(b). Note that upon cooling below 100 K, the resistance of the samples (on STO and on LAO) is not measurable due to the limitation of the voltmeter. The charge-ordering temperature ($T_{\text{CO}} \sim 270$ K) is characterized by a kink in resistivity and appears to be same for both types of films. The opposite nature of stress in the films of PCMO on STO and LAO is clearly observed in the magnetic-field dependence of the resistivity vs temperature. For example, the ZFC resistivity of the PCMO/STO sample at 9 Tesla [Fig. 1(a)] is thermally activated on cooling below room temperature down to 120 K. A metallic-like behavior is observed in the temperature range of 120 K to 65 K and below 65 K, the thermally activated behavior reappears. As previously stated, the situation (in the presence of an applied magnetic field) is different for PCMO/LAO. The resistivity of this sample on cooling in 7 Tesla magnetic field below room temperature shows thermally activated behavior down to ~ 160 K with $E_a \sim 0.31$ eV, and then below 160 K the resistivity is metal-like down to 10 K. Similar major differences have already been observed in these compositions of thin films and explained by the difference in the orientation of the thin films with respect to the substrate.^{11,12} Another difference between both substrates is observed in magnetic measurements [Figs. 1(c) and 1(d)]. The magnetic moment (FC and ZFC) of PCMO on STO decreases slowly on heating from 10 K to 190 K. The magnetic moment then decreases slowly above 220 K up to room temperature. A qualitatively similar behavior of the magnetization of the PCMO films

deposited on LAO is seen. Denoted by a kink in the temperature-dependence of the magnetic moment, the Néel temperature (T_N) of the PCMO films on LAO and STO is 170 K and 190 K, respectively (see Fig. 1). This is close to the value for bulk samples ($T_N \sim 175$ K).¹⁴ These results indicate that there are some significant differences in both the magnetotransport and magnetization data of PCMO on STO and LAO (Fig. 1) as a result of the substrate-induced strains.

Though the transport measurements in thin films show melting of the charge-ordered state at a lower magnetic field as compared to that of the bulk (for details, see Refs. 11 and 12), this is not an artifact of the Joule heating as these measurements have been performed at a very low current ($10 \mu\text{A}$). Different approaches have been used in the literature to minimize Joule heating in such measurements. Some of these are:

(i) Limit the width and thickness of the samples to a few microns. This approach can give erroneous results as the characteristic correlation length of the ordered/disordered state in CO manganites is quite large.^{15,16}

(ii) An external load resistor in series with the sample is used as a current limiting device.^{4,15-17} This arrangement limits the maximum electric field that can be applied across the sample with a power supply of moderate voltage output (~ 100 V).

(iii) A pulsed (~ 1 s) current technique has also been used to reduce Joule heating. However, the pulsed mode is not suitable to study hysteretic behavior. Since the electrical conduction in these systems depends strongly on the current history, the hysteretic behavior may change if the current is switched on and off during cycling. In order to avoid some of these complications, we have first reduced the strength of the CO state through application of a magnetic field and then measured the charge transport at moderate electric field.

Figure 2(a) shows the temperature dependent resistivity $\rho(T)$ of a ~ 800 Å thick PCMO film on LAO measured at $10 \mu\text{A}$ for different values of the in-plane magnetic field. In the presence of a 5 Tesla magnetic field, the resistivity of the sample upon cooling below room temperature shows thermally activated behavior down to 120 K and then becomes metal-like in the temperature window of 65 K to 120 K. Below 65 K the resistivity is again thermally activated. A qualitatively similar behavior with a wider metal-like window and lower magnitude of resistivity is seen at higher magnetic fields (>5 Tesla). Such features are typical of a CO system where an external magnetic field destroys the CO state and induces a metallic behavior³ and have already been observed in thin films of PCMO.^{11,12}

A difficult problem one faces inevitably when measuring voltage-current characteristics is the Joule heating of the samples.¹⁸ Thus, prior to performing these current-voltage (I - V) measurements, we have estimated the suitable limit for the electric field from a simple calculation of the increase in the sample temperature due to Joule heating. The increase in sample temperature (ΔT) when the current I flows through it was estimated by taking into account the heat dissipation in the sample and heat conduction by the substrate. Assuming the substrate is anchored to the isothermal base of the

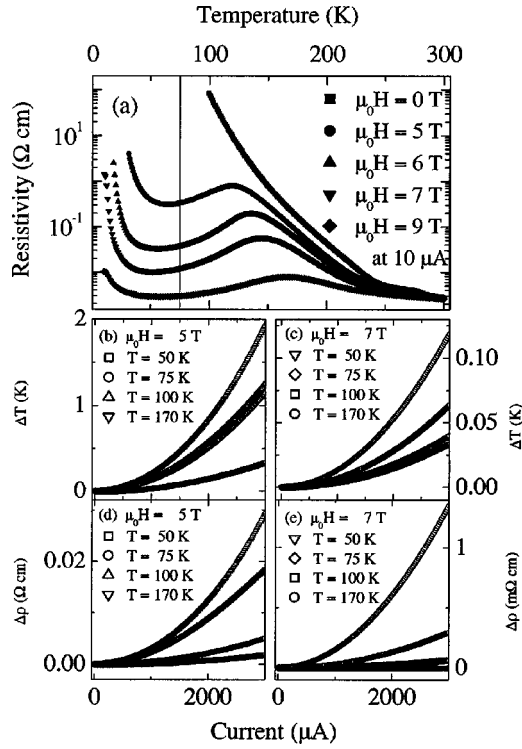


FIG. 2. Panel (a) shows the zero-field-cooled temperature dependent resistivity of PCMO deposited on (001) oriented LAO at various magnetic field with $10 \mu\text{A}$ driving current. Lower panels (b) and (c) show the estimated change in the resistivity while panel (d) and (e) show the estimated change in the sample temperature due to the driving current in the sample at different temperature at 5 Tesla and 9 Tesla magnetic field, respectively.

PPMS, the increase in temperature can be approximated as $\Delta T \sim 2P_l/\kappa_{\text{sub}}$, where P_l is the power dissipated per unit length of the sample and κ_{sub} is the thermal conductivity of the substrate. The increase in temperature of the sample at a constant thermal base temperature (T) can be expressed as $\Delta T(T, I) = (2I^2\rho(T + \Delta T)/S\kappa_{\text{sub}}(T + \Delta T))$, where S is the cross section of the sample.¹⁸ The κ_{sub} of LAO at 77 K and 197 K is $0.186 \text{ W cm}^{-1} \text{ K}^{-1}$ and $0.143 \text{ W cm}^{-1} \text{ K}^{-1}$, respectively.¹⁹ Even though the thermal conductivity of LAO varies with temperature, we have assumed an average value of $\kappa_{\text{sub}} = 0.15 \text{ W cm}^{-1} \text{ K}^{-1}$, in the temperature range of 10–170 K. Using the experimental values $\rho(T)$ and $\kappa_{\text{sub}} = 0.15 \text{ W cm}^{-1} \text{ K}^{-1}$, the calculated temperature rise (ΔT) at different temperatures for the sample ($0.5 \times 0.1 \times 8.10^{-6} \text{ cm}^3$) on LAO at 5 Tesla and 7 Tesla is shown in Figs. 2(b) and 2(c), respectively. The corresponding increase in resistivity inferred from Fig. 1 [panel (a)] is shown in panels d and e, respectively. While $\Delta T(T, I)$ is quadratic in current, its value remains small ($< 2 \text{ K}$) even when $\sim 3000 \mu\text{A}$ current passes through the sample. The corresponding changes in the resistivity are also small [less than $0.2 \Omega \cdot \text{cm}$ under a magnetic field of 5 T at 170 K; see Fig. 2(d)]. Similar calculations were performed for PCMO films on STO. In this case, however, the calculated increase in temperature is much larger. This is due to the high resistivity of PCMO on STO ($10^{-1} \Omega \cdot \text{cm}$) in the range of 100–150 K

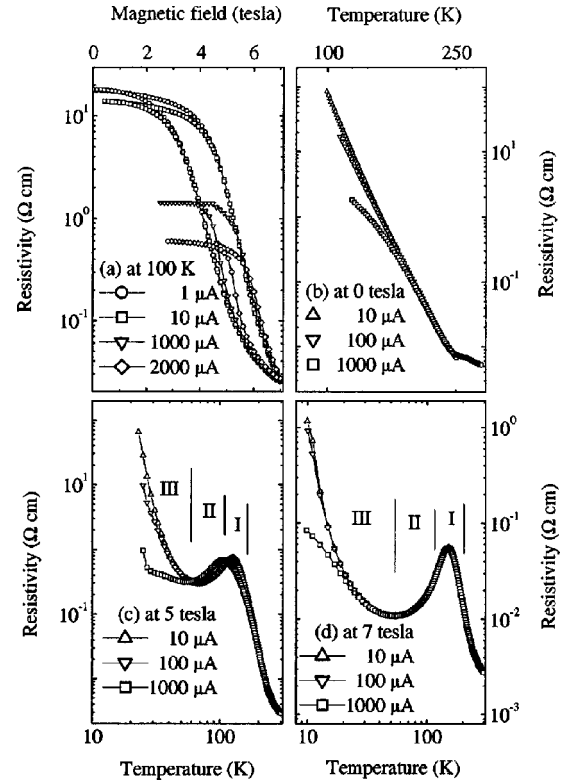


FIG. 3. Panel (a) shows the zero-field-cooled resistivity of the same sample at various current as the magnetic field increases from 0 to 7 Tesla and then decreases from 7 Tesla to 0. Panels (b), (c), and (d) show the zero-field-cooled temperature dependent resistivity of PCMO on LAO at 0, 5, and 7 Tesla magnetic field at 10, 100, and 1000 μA driving current.

even under the application of a 9 Tesla field [see Fig. 1(a)]. For this reason, we focus our study only on the sample grown on LAO.

To understand the collective effect of magnetic field and electric field on transport properties, we have measured the resistivity of a PCMO film on LAO at 100 K for different values of magnetic field (from 0 to 9 T) and various driving currents (from $1 \mu\text{A}$ to $2000 \mu\text{A}$). The magnetic field dependence of resistivity at 100 K for 1, 10, 1000, and 2000 μA currents is shown in Fig. 3(a). The resistivity measured at $1 \mu\text{A}$ first decreases slowly as the magnetic field is increased from zero to a critical value $H^* \sim 3.5$ Tesla, and then drops rapidly until reaching the maximum field of 7 Tesla. As the magnetic field is reduced from 7 Tesla, the resistivity is irreversible up to the field $H_{\text{irr}} \sim 1.5$ Tesla and then becomes reversible. This hysteretic behavior is typical of a first order transition as previously observed from CO compounds.³ For higher values of current, the zero-field and field dependent resistivity shows the following four characteristics:

- (i) Below 150 K, the resistivity in zero-field is lower for higher currents [up to $1000 \mu\text{A}$; see Fig. 3(b)];
- (ii) The magnitude of resistivity is lower;
- (iii) H_{irr} shifted to the higher fields;
- (iv) The MR at $2000 \mu\text{A}$ current is less than the MR with a current below $2000 \mu\text{A}$.

The combined effect of electric field and magnetic field on ZFC resistivity of PCMO as a function of temperature is

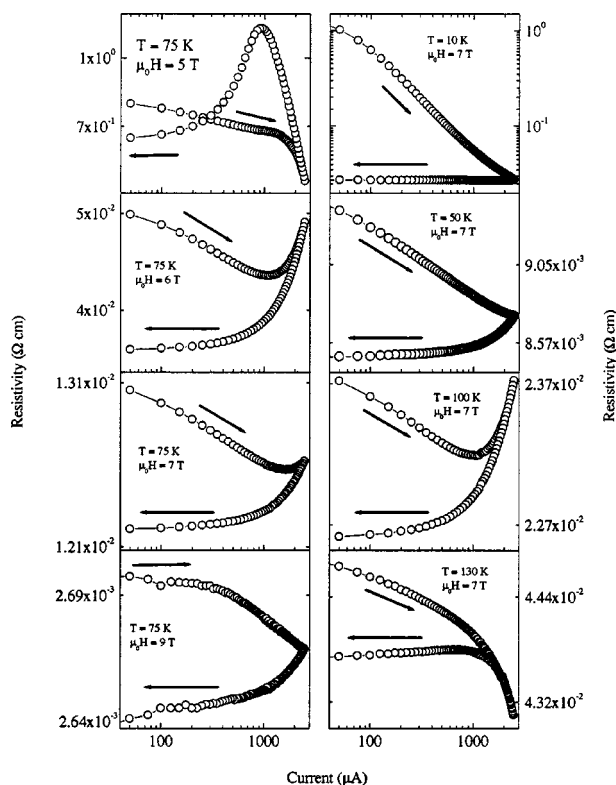


FIG. 4. Left-hand panel shows the zero-field-cooled resistivity of PCMO on LAO at 75 K at various magnetic field as the current increases from 1 μA to 2500 μA followed by a decrease to 1 μA . Right-hand panel show the zero-field-cooled resistivity of the same sample at 7 Tesla magnetic field at 10, 50, 100, and 130 K, respectively, as the current increases from 1 μA to 2500 μA and then decreases from 2500 μA to 1 μA .

shown in Figs. 3(c) and 3(d). In fact, three regimes are observed (I, II, and III). At 5 Tesla and 10 μA current, the $\rho(T)$ below room temperature is thermally activated down to 125 K (regime I), and in the temperature window of 65 K to 125 K, it has metal-like behavior (regime II). Below 65 K, the $\rho(T)$ is increasing upon cooling (regime III). However, a large drop in $\rho(T)$ is seen with the increasing current in this temperature range (10–65 K). A qualitatively similar behavior of resistivity with the increasing current is seen in 7 Tesla magnetic field [Fig. 3(d)]. Although the CO phase in these systems phase is destroyed by the magnetic field, the effect of electric current on the resistivity at low temperatures is still prominent.

In order to address this nonlinear transport, we have carried out isothermal measurement of resistivity as a function of current. The current-dependence of resistivity $\rho(I)$ of PCMO on LAO at 75 K in the presence of 5, 6, 7, and 9 Tesla is shown in the left-hand panel of Fig. 4. The resistivity at 5 Tesla first decreases slowly up to 1000 μA and then decreases much more rapidly. On decreasing the current below 2500 μA , the $\rho(I)$ goes through a peak at 950 μA where the resistivity is higher than the value seen in the current increasing branch. On lowering the current, the resistivity decreases and crosses the current increasing branch at 300 μA . The behavior of $\rho(I)$ at 6 Tesla is significantly dif-

ferent. Here the resistivity goes through a minimum at a critical current ($I_C \sim 1000 \mu\text{A}$) and then increases rapidly with the increase in current up to 2500 μA . The resistivity-current decreasing of the branch $\rho(I)$ is lower than the forward branch over the entire range of current. The hysteretic behavior of $\rho(I)$ at 7 Tesla is qualitatively similar, with a higher I_C ($\sim 1500 \mu\text{A}$). However, at 9 Tesla the resistivity continues to drop with current without any signatures of I_C until reaching the maximum current of 2500 μA . The $\rho(I)$ of the same sample at 10, 50, 100, and 130 K and 7 Tesla field is shown in the right-hand panel of Fig. 4. The hysteretic behavior of resistivity as the current is swept from 0 to 2500 μA and back to zero, is seen at all temperatures with some subtle differences.

The observed behavior of resistivity of PCMO films as a function of temperature, current and strength of magnetic field can be understood as follows. The thermally activated behavior at the lowest temperature in the ZFC $\rho(T)$ at 7 Tesla as seen in Fig. 1(b) indicates the presence of a charge-order gap. However, a long range CO state does not form when we cool the sample in the 7 Tesla field. While the magnetic field promotes the growth of ferromagnetic clusters and reduces spin dependent intercluster scattering, the electric field increases the ferromagnetic fraction as shown by the increase of H_{irr} , H^* and the reduction of resistivity with increasing current as seen in Fig. 3(a).

These nonlinear behaviors of the resistivity with current suggest the presence of other mechanisms. To understand this nonlinear transport in PCMO, we have measured the $\rho(I)$ in different regions of temperature in the presence of a magnetic field. The isothermal $\rho(I)$ shows hysteretic behavior and it is symmetric with current provided the sample is cooled from the room temperature to the desired temperature to measure both the directions of current. In the paramagnetic and insulating state, $\rho(I)$ decreases slowly with temperature and is reversible with current. The hysteretic behavior of $\rho(I)$ at $T < T_C$ (Fig. 4) distinguished three zones in the $\rho(T)$ curve, the temperature zone close to the metal-to-insulator ($M-I$) transition, metal-like $\rho(T)$ zone, and low temperature insulating zone. These three zones have been marked as region (I), region (II), and region (III), respectively, and are shown in Fig. 3. In Fig. 4, region (I) is observed at 130 K and 7 T whereas region (III) corresponds to 10 K and 50 K at 7 T. Region (II) is seen at 75 K with a magnetic field from 5 to 9 T. On reducing current, the resistivity stays relatively constant. Note that at zero current, the resistivity is always lower than the initial one.

These data can be explained using the phase-separation (PS) scenario, which consists of a fine mixture of the two competing ground states, the ferromagnetic (FM) metallic state and the charge/orbital-ordered insulator one.^{20–23} The competition between the FM metallic state due to the double-exchange and the antiferromagnetic (AFM) nonmetallic state, due to the 1:1 ordering of $\text{Mn}^{3+}/\text{Mn}^{4+}$, has been seen in $\text{RE}_{1-x}\text{Ca}_x\text{MnO}_3$ ($\text{RE}=\text{Pr}, \text{Nd}$).²⁴ Thus, we have assumed that our PCMO film is a PS system. This is reasonable based both on our previous experiments using electron spin resonance made on the same film composition²⁵ and also on the magnetotransport measurements of films which indicate that the

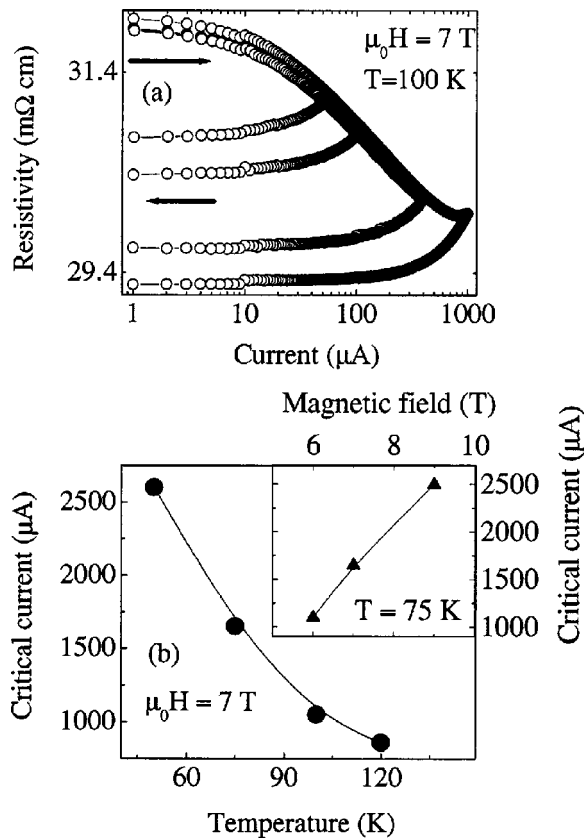


FIG. 5. Panel (a) shows the zero-field-cooled resistivity of PCMO on LAO at 7 Tesla magnetic field at 100 K as the current increases from 1 μA to a different higher value followed by a decrease to 1 μA . Panel (b) shows the critical current at 7 Tesla magnetic field at different temperatures. The critical current at different magnetic field at 75 K is shown in the inset of panel (b). The critical current I_C is the excitation current at which the MR starts to be nonhysteretic in Fig. 4.

metal-like regions are growing and that the insulator-like regions are, simultaneously, shrinking in the presence of an applied magnetic field [see Figs. 1(a), 1(b), and 2(a)]. If one compares the three different regions (I), (II), and (III), the situation of the ground states is different, due to the presence of magnetic field and the different temperatures ranges³ [this is observed in the value of resistivity in Figs. 3(c) and 3(d)]. For example, from the magnetic point of view, in region (I), the film is in the PM state with a short range ordering²¹ whereas in region (II), the AFM (COI) regions are present in the FM (metal) matrix. In region (III), the AFM (COI) state is partially ordered. The picture of the mechanism of current-induced is as follows. When current is applied in the sample, it drives the electrons towards the lower potential energy, which changes the effective electron-electron interaction and modifies the charge distribution in the metal-like stripe regions that stays when the current is reducing to 1 μA . This is evidenced in Fig. 5(a), where the resistivity shows a hysteretic behavior as a function of the applied current. Depending on the values of the resistance, i.e., the portion of metallic phase with respect to the insulating one, the current will stabilize local thermal regions. When the current is reduced, the sample is (magnetic) field cooled and remains in its small

resistivity value as one can see in Fig. 1. This explains why the resistance decreases as the current is reduced. Using this model, the current-dependence of the resistivity in the three different regions can now be explained.

In region (I), the sample is mostly metallic, but the insulating regions are growing due to the applied magnetic field and the value of temperature [130 K, which is just below the insulator-to-metal transition in Fig. 2(a)]. Below 1000 μA , the hysteretic behavior and the decrease of resistivity are observed, indicating a melting of the CO state. However, the changes are very small confirming that the CO state is almost completely melted with an applied magnetic field of 7 T. Above 1000 μA , the reversal resistivity drops are due to the homogeneous Joule heating.

In region (II), the resistivity increases as temperature increases (under applied magnetic field). In addition, the metallic phase is growing as the magnetic field increases, a signature of the melting of the CO state.³ When the current is below 1000 μA , most of the CO has been melted although the value of the magnetic field is not sufficient to melt it completely (at least below 9 T). Thus, the applied current will melt the regions that were still CO. Since the fraction of these regions is very small, the decrease is very small. On the contrary, with a magnetic field of 9 T, the resistivity is constant under applied current up to 500 μA confirming that the CO is completely melted in accordance with previous reports.^{11,12} Surprisingly above 1000 μA , the resistivity increases as the current increases. This increase can be explained with thermal instabilities because in this region, when the temperature increases, the resistivity increases as well.

In region (III), most of the sample is insulating because the magnetic field is not sufficient to completely melt the CO state.^{11,12} When the current is applied (up to 1000 μA), it also modifies the charge distribution of the CO state, increasing the metallic regions.²⁶ However, the magnetic field will induce some metallic regions that, as seen previously, will heat locally.

The situation of the $\rho(I)$ at 75 K and 5 T is more complicated because it is just at the boarder between the two regions (I) and (II). On increasing the current, there is a decrease and then a jump at 1000 μA due to Joule heating. In fact, the heating is so important, that the sample is crossing the metal-to-insulator region [see Fig. 2(a)]. On decreasing the current, it will follow that curve and this results in the peak in the $\rho(I)$.

In fact, in the different regions the resistivity decreases as the current increases up to critical value (I_C), and then either increases or decreases rapidly (depending on the values of resistivity). The behavior can thus be separated into two zones, below and above I_C which can be considered as a threshold. In Fig. 5(b), we have reported this critical current which separates the two behaviors (thermal instabilities and nonlinear conduction). This limit is an image of the shape of the temperature and magnetic field dependence of the resistivity.

We also have noted that the effect of current-induced decrease of resistivity in manganite-based compounds is not a particular case of the thin films and has already been studied in bulk samples.²⁶⁻²⁸ However, in some cases, the values of

current-inducing a metallic behavior were much higher (on the order of mA or above) and the real effects are probably obscured by Joule heating.^{27,28} In other cases,²⁶ the values of the current are lower compared to our values (on the order of nA) which makes the comparison difficult. In this latter case, they clearly observed a first order transition from a charge-ordered state to a metallic state.

In conclusion, we have studied the effects of currents on the transport properties of $\text{Pr}_{0.5}\text{Ca}_{0.5}\text{MnO}_3$ thin films grown on LaAlO_3 and SrTiO_3 substrates. We have performed detailed measurements of the resistivity as a function of current and temperature in the presence or absence of a magnetic field. Our data reveal that two mechanisms, local heating and nonlinear conduction, are observed depending on tempera-

ture and the value of the resistivity. The origin of this behavior is explained with a model based on local thermal instabilities in the metallic percolation regions resulting from the phase-separation system and a modification in the long range charge-ordered state.

We gratefully acknowledge the financial support of Centre Franco-Indien pour la Promotion de la Recherche Avancée/ Indo-French Centre for the Promotion of Advance Research (CEFIPRA/IFCPAR) under Project No. 2808-1. We also thank Dr. H. Eng, Dr. A. Wahl, and Dr. A. Maignan for careful reading of the article and helpful discussions during this work.

*Electronic address: prellier@ensicaen.fr

¹A. P. Ramirez, *J. Phys.: Condens. Matter* **9**, 8171 (1997).

²W. Prellier, Ph. Lecoeur, and B. Mercey, *J. Phys.: Condens. Matter* **13**, R915 (2001).

³C. N. R. Rao, A. Arulraj, A. K. Cheetham, and B. Raveau, *J. Phys.: Condens. Matter* **12**, R83 (2000).

⁴A. Asamitsu, Y. Tomioka, H. Kuwahara, and Y. Tokura, *Nature (London)* **388**, 50 (1997).

⁵Ayan Guha, Arindam Ghosh, A. K. Raychaudhuri, S. Parashar, A. R. Raju, and C. N. R. Rao, *Appl. Phys. Lett.* **75**, 3381 (1999).

⁶Y. Tokura and N. Nagaosa, *Science* **288**, 462 (2000).

⁷J. Stankiewicz, J. Sese, J. Garcia, J. Blasco, and C. Rillo, *Phys. Rev. B* **61**, 11236 (2000).

⁸S. Srivastava, N. K. Pandey, P. Padhan, and R. C. Budhani, *Phys. Rev. B* **62**, 13868 (2000).

⁹S. Mercone, A. Wahl, Ch. Simon, and C. Martin, *Phys. Rev. B* **65**, 214428 (2002).

¹⁰V. Markovich, I. Fita, A. I. Shames, R. Puzniak, E. Rozenberg, C. Martin, A. Wisniewski, Y. Yuzhelevskii, A. Wahl, and G. Gorodetsky, *Phys. Rev. B* **68**, 094428 (2003).

¹¹W. Prellier, A. M. Haghiri-Gosnet, B. Mercey, Ph. Lecoeur, M. Hervieu, Ch. Simon, and B. Raveau, *Appl. Phys. Lett.* **77**, 1023 (2000).

¹²W. Prellier, Ch. Simon, A. M. Haghiri-Gosnet, B. Mercey, and B. Raveau, *Phys. Rev. B* **62**, R16337 (2000).

¹³Z. Jirak, S. Krupicka, Z. Simsa, M. Doulka, and S. Vratislma, *J. Magn. Magn. Mater.* **53**, 153 (1985).

¹⁴N. Lavrov, I. Tsukada, and Yoichi Ando, *Phys. Rev. B* **68**, 094506 (2003).

¹⁵M. Fiebig, K. Miyano, Y. Tomioka, and Y. Tokura, *Science* **280**, 1925 (1998).

¹⁶S. Yamanouchi, Y. Taguchi, and Y. Tokura, *Phys. Rev. Lett.* **83**, 5555 (1999).

¹⁷K. Hatsuda, T. Kimura, and Y. Tokura, *Appl. Phys. Lett.* **83**, 3329 (2003).

¹⁸A. N. Lavrov, I. Tsukada, and Y. Ando, *Phys. Rev. B* **68**, 094506 (2003).

¹⁹Peter C. Michael, John U. Trefny, and Baki Yarar, *J. Appl. Phys.* **72**, 107 (1992).

²⁰For a review, see A. Moreo, S. Yunoki, and E. Dagotto, *Science* **283**, 2034 (1999).

²¹M. Uehara, S. Mori, C. H. Chen, and S.-W. Cheong, *Nature (London)* **399**, 560 (1999); S. Mori, T. Asaka, and Y. Matsui, *J. Electron Microsc.* **51**, 225 (2002).

²²L. Zhang, C. Israel, A. Biswas, R. L. Greene, and A. Lozanne, *Science* **298**, 805 (2002).

²³M. Fäth, S. Freisem, A. A. Menovsky, Y. Tomioka, J. Aarts, and J. A. Mydosh, *Science* **285**, 1540 (1999).

²⁴T. Tomioka, A. Asamitsu, H. Kuwahara, Y. Moritomo, M. Kasai, R. Kumai, and Y. Tokura, *Physica B* **237–238**, 6 (1997).

²⁵S. de Brion, G. Storch, G. Chouteau, A. Janossy, W. Prellier, and E. Rauwel-Buzin, *Eur. Phys. J. B* **33**, 413 (2003).

²⁶A. Asamitsu, Y. Moritomo, Y. Tomioka, T. Arima, and Y. Tokura, *Nature (London)* **388**, 50 (1997).

²⁷S. Parashar, L. Sudheendra, A. R. Raju, and C. N. R. Rao, *J. Appl. Phys.* **95**, 2181 (2004).

²⁸L. Sudheendra and C. N. R. Rao, *J. Appl. Phys.* **94**, 2767 (2003).